



LIBRARY Michigan State University

This is to certify that the thesis entitled

A SELF-TUNING SEMI-ACTIVE HELMHOLTZ RESONATOR

presented by

Swaroop Mannepalli

has been accepted towards fulfillment of the requirements for the

M.S. degree in Mechanical Engineering

Date

PLACE IN RETURN BOX to remove this checkout from your record. TO AVOID FINES return on or before date due. MAY BE RECALLED with earlier due date if requested.

DATE DUE	DATE DUE	DATE DUE
	,	

6/01 c:/CIRC/DateDue.p65-p.15

A Self-Tuning Semi-Active Helmholtz Resonator

Ву

Swaroop Mannepalli

A THESIS

Submitted to
Michigan State University
in partial fulfillment of the requirements
for the degree of

MASTER OF SCIENCE

Mechanical Engineering

2003

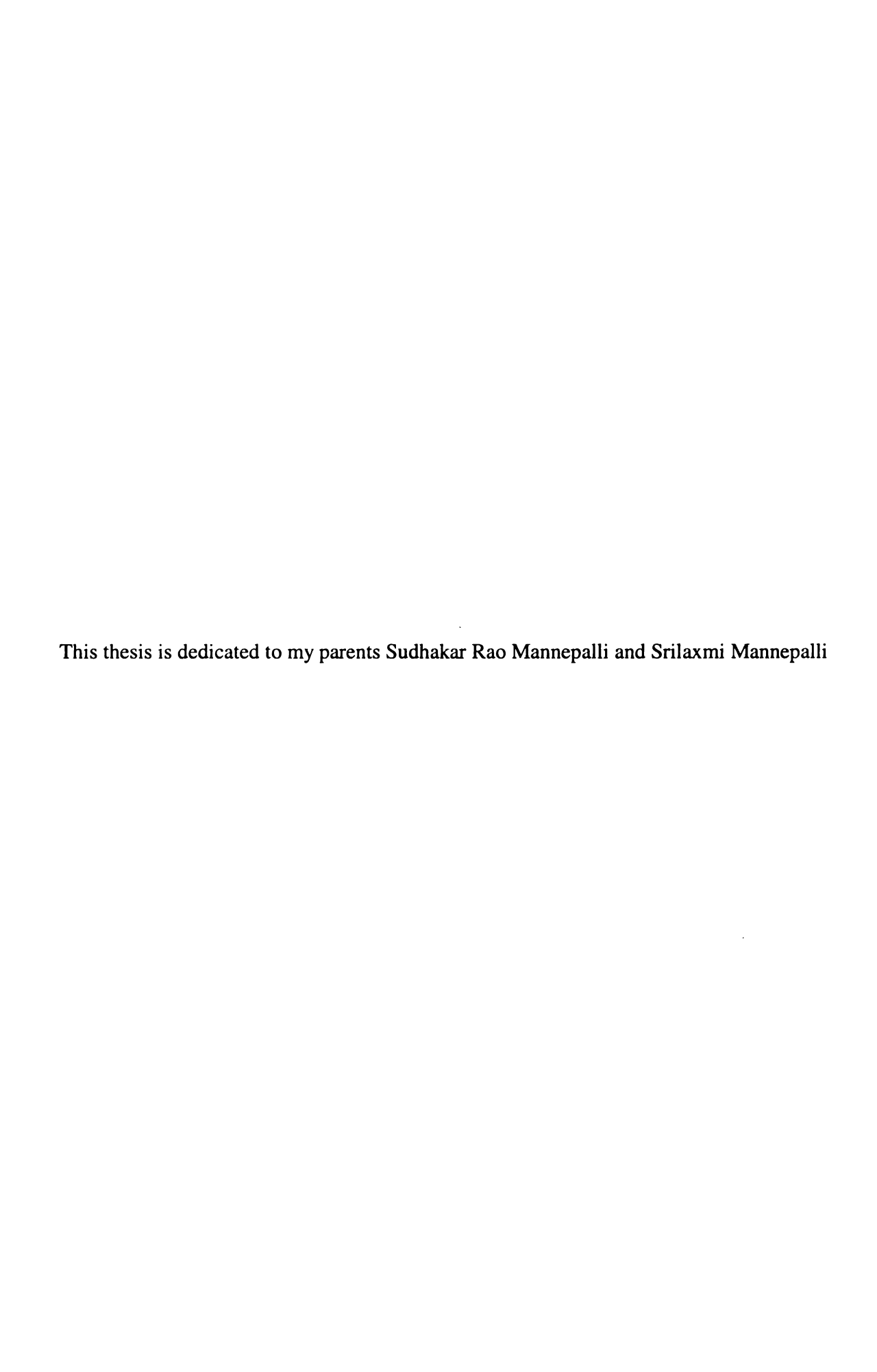
ABSTRACT

A SELF-TUNING SEMI-ACTIVE HELMHOLTZ RESONATOR

Bv

Swaroop Mannepalli

Helmholtz resonators are commonly used to reduce the sound transmitted through the acoustic systems such as vehicle exhaust and industrial ducting systems. These Helmholtz resonators are tuned to a particular frequency at which they eliminate noise. These are not effective if the disturbance frequency varies in time. Active tuning of these resonators has been achieved in different ways and these systems were called semi active Helmholtz resonators (SHR). All previous methods used a computer for tuning of the resonator. This work presents a more compact control system which can modify the acoustic response of the resonator online with self-tuning. A closed loop adaptive control strategy has been adopted for this system (SHR). This SHR uses gain scheduling to tune the device online and track a disturbance signal. The system consists of a static Helmholtz resonator designed to enforce the nominal resonance and a feedback control system with preprogrammed microcontroller to enforce the tuning of the resonator. This improved feedback system has the advantage of self-tuning and low power consumption. The volume and weight of the entire system reduced by about 80%. The microcontroller used in this system (SHR) reduced the cost by 90%. Noise attenuation of approximately 10 - 20 dB was achieved with this system.



ACKNOWLEDGEMENTS
I would like to thank Dr.Clark Radcliffe for his continued support throughout my work.
Special thanks to Sean Vidanage for his assistance and suggestions. I would also like to
thank my room mates for their active support.

TABLE OF CONTENTS

ABSTRACTi	ii
TABLE OF CONTENTS	v
LIST OF FIGURES	⁄i
LIST OF TABLESvi	ii
LIST OF ABBREVIATIONSi	X
1 Introduction	1
2 Adaptive Semi Active Helmholtz Resonator	4
2.1 The Semi active Helmholtz Resonator	4
2.2 Analytical Helmholtz Resonator Model	6
2.3 Actuator and its effect on SHR	2
2.4 Controller design with actuator dynamics	4
2.5 Experimental Model Validation with DSP Board	7
3 Hybrid Controller	1
3.1 Hybrid control system2	1
3.2 Analog Circuit	2
3.3 Microcontroller	4
3.4 Frequency estimation and self-tuning	5
3.5 Experimental Results	6
4 Conclusions	2
Bibliography3	3
Appendix A3	5
Appendix B3	7

LIST OF FIGURES

Figure 1	Helmholtz resonator connected to a duct	2
Figure 2	SHR connected to a primary acoustic system	5
Figure 3	Experimental SHR connected to a primary acoustic system	6
Figure 4	Ideal Helmholtz Resonator	8
Figure 5	Frequency Response $Q_I(s)/P_I(s)$ of the Helmholtz resonator $(V = 6.71 \times 10^{-4})$	
m^3 , L	$_{ve}$ = 4.00 cm and S=2.54×10 ⁻⁴ m ²)	9
Figure 6	Helmholtz resonator with complex impedance boundary condition	.10
Figure 7	Complimentary Root locus for (a) K_p with $K_i = 0$ (b) K_i with $K_p = 0$.12
Figure 8	Closed loop coupled model of the SHR	.15
Figure 9	Simulated frequency response of the transfer function $P_2(s)/D_1(s)$ for the SHI	3
with	ω_n =100Hz, 114Hz, 127Hz, 140Hz and 153Hz	.16
Figure 10	Experimental setup using the digital signal processor	.18
Figure 11	Comparison of K_p and K_i Vs ω_n	.19
Figure 12	Experimental frequency response $P_2(s)/D_1(s)$ for gain scheduling controller	
using	the Dspace board with $\omega_n = 100$, 126, 137 and 164 Hz	.20
Figure 13	Hybrid Controller (a) Schematic (b) Experimental	.22
Figure 14	The complete analog circuit	.23
Figure 15	Schematic of the experimental setup using microcontroller	.26
Figure 16	Experimental frequency response $P_2(s)/D_I(s)$ for gain scheduling controller	
with	$\omega_n = 100, 112, 135, 154$ and 178 Hz and with gains set to zero	.28

Figure 17 Experimental Sound pressure measured in the resonator cavity (top channel)
and the output of the acoustic duct (bottom channel) at 132 Hz (a) with controller off
(b) with controller on30
Figure 18 Experimental Sound pressure measured in the resonator cavity (top channel)
and the output of the acoustic duct (bottom channel) at 147 Hz (a) with controller off
(b) with controller on
Figure 19 Analog Circuit
Figure 20 Self-Tuning Algorithm

LIST OF TABLES

Table 1	Analytical model parameter values	14
Table 2	Controller gains for $K_{amp} = 1$, $\xi = 0.10$ and $S_{mic} = 0.04$	16
Table 3	Controller gains for analog circuit	28
Table 4	Analog Circuit component values	35

LIST OF ABBREVIATIONS

Upper Case	5
	acoustic compliance (m ⁵ /N)
D_1	
	.controller transfer function
<i>G2(s)</i>	.actuator transfer function
I_a	acoustic inertia
I_c	coil inductance
<i>K</i> _{amp}	amplifier gain
K_i	
K_p	.proportional gain
	.mutual inductance (H)
P_1	pressure at the resonator neck inlet (N/m ²)
	pressure inside the resonator cavity
	.volume velocity in the resonator neck (m ³ /s)
	.volume velocity in the resonator cavity (m ³ /s)
	acoustic radiation loss
R_c	speaker coil resistance
S	
	.speaker face area (m ²)
	semi-active helmholtz resonator
	microphone sensitivity (Volts/Pa)
	volume of the resonator cavity (m ³)
Lowercase	
bl	electromechanical coupling factor (N/amp)
<i>c</i> ₀	speed of sound in air (m/s)
<i>e</i> _n	primary coil voltage (Volts)
	primary coil current (amp)
<i>a</i> ₁	volume displacement in resonator neck (m ³)
q_2	volume displacement of speaker (m ³)
S	
	······································
Greek	
λ	magnetic flux
ξ	
00	density of air (Kg/m ³)
ν	natural frequency (rad/s)
ω_n	natural frequency (raws)

1 Introduction

Acoustic noise has long been recognized as a source that can have adverse effects on human life. For example, low frequency noise in the range of 200 Hz and below has been found to cause structural vibration. Passive techniques such as the use of absorbent materials have little effect on the low frequency noise and tend to make the system more bulky. Various attempts have been made to solve this problem, one of which is the design of a semi active Helmholtz resonator (SHR). Helmholtz resonators are commonly used to reduce the sound transmitted through acoustic systems such as vehicle exhaust and industrial ducting systems. One advantage of the Helmholtz resonator is its simplicity. The Helmholtz resonator has the shape of a bottle. The size of the opening, the length of the neck and the volume of air trapped in the chamber govern the resonant frequency (Temkin, 1981). They must be tuned precisely to achieve significant noise attenuation. They function by reflecting sound back to the source. The resonator's effective frequency range is narrow and fixed. Changes in the excitation frequency and environmental conditions affect the performance of this device. Due to the limitations imposed by this passive device, active noise control methods have been the subject of interest. The main advantage of active noise control over passive control schemes is the implicit adaptability of the control system to changing environments and excitations.

Active noise cancellation uses the interference of acoustic waves so that when a secondary source of noise is introduced destructive interference occurs leading to a reduction of the unwanted noise. This is achieved by artificially generating a secondary

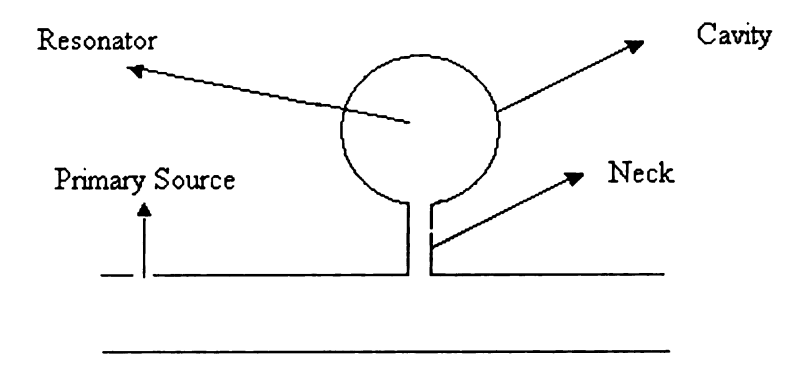


Figure 1 Helmholtz resonator connected to a duct

source of noise. This secondary source produces a wave in anti-phase with the unwanted noise so that when the two waves are superimposed on each other, the noise is attenuated.

The Helmholtz resonator (Figure 1) is a device that produces an anti-phase wave at its resonant frequency. This resonant frequency of the device could be varied by active tuning of the resonator to produce an active noise cancellation system.

Active tuning of the Helmholtz resonator can be achieved by varying the resonator neck dimensions, cavity volume or both. Active tuning of the Helmholtz resonators has been achieved by different methods. Koopman and Neise (1982) achieved active tuning by changing the cavity volume by a movable Teflon piston. Lamancusa (1987) proposed two configurations for variable volume. One was achieved by using a piston and for the second configuration, several discreet volumes were utilized by manipulating closable partitions in the cavity. Little et al (1994) proposed the use of an electro-rheological fluid valve to tune the resonator by varying the neck cross-sectional area. Bedout (1997) proposed the use of a variable volume resonator by rotating a radial internal wall inside the resonator cavity. All the methods used above involved significant

mechanical complexity. Radcliffe and Birdsong (1999) proposed a simple, closed loop adaptive control strategy. Using a simple electromechanical actuator modifies the acoustic response of the resonator. This method of tuning the resonator eliminates the mechanical complexity involved and the response to variable frequency is made quicker. All the methods described above used a Personal computer to realize the control algorithm.

In the new work described here a simpler control system implementation has been designed, which modifies the acoustic response of the resonator online with self-tuning. The system consists of a Helmholtz resonator designed to enforce nominal resonance and a hybrid feedback control system that provides variable acoustic impedance. The feedback control system consists of a preprogrammed microcontroller that selects the controller gains based on the frequency of the unwanted noise. Selected controller gains are used to modify the resonant frequency of the Helmholtz resonator with the help of a speaker acting as an actuator. A microphone that senses the pressure in the cavity and drives the actuator through a controller that provides an appropriate magnitude and phase to the actuator velocity. This magnitude and phase relationship can be related to acoustic impedance. The acoustic impedance of the Helmholtz resonator can be defined by the ratio of the pressure at the resonator inlet to the volume velocity through the inlet. Changing the cavity wall impedance can change this acoustic impedance of the Helmholtz resonator. This shows that the overall acoustic impedance is a function of resonators dimensions and controller gains, which can be changed online in order to generate variable impedance to remove the unwanted noise (Birdsong, 1999).

2 Adaptive Semi Active Helmholtz Resonator

An analytical model of the semi-active Helmholtz resonator and its validation are presented. The model shows that the acoustic impedance on the interior wall of the resonator cavity can be modified. This change in acoustic impedance is achieved by changing the controller gains in order to modify the overall acoustic response of the system. A stable set of controller gains was derived using the model based controller design.

2.1 The Semi active Helmholtz Resonator

The SHR (Figure 2) consists of a Helmholtz resonator with the addition of a pressure sensor, actuator H(s) and a controller G(s). The Helmholtz resonator is a device that consists of an enclosed volume connected to a narrow neck, like the shape of a bottle. The resonant frequency of the Helmholtz resonator is defined by the physical dimensions of the resonator. In order to retune the resonant frequency of this device, a speaker H(s) is used as an actuator which generates a volume flow rate inside the resonator cavity. This speaker is driven by a controller G(s), the input of which is the pressure inside the resonator cavity sensed through the pressure sensor.

The Helmholtz resonator is used in attenuating noise. When driven by a pressure from the primary acoustic system, the resonator responds with a large magnitude volume velocity through the system resonator neck, which is in phase with the pressure. This creates a pressure release boundary condition, which inverts and reflects the incident pressure wave, thus reducing the transmitted pressure wave (Pierce, 1981).

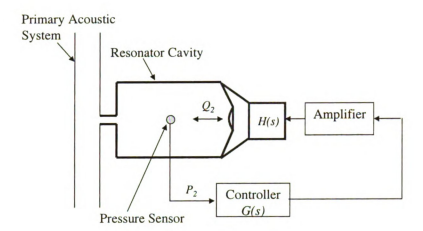


Figure 2 SHR connected to a primary acoustic system

This design has two important benefits. The first being, when the controller is turned off, the system resonates at its nominal resonant frequency defined by the physical dimensions of the Helmholtz resonator. Since these dimensions can be designed to meet the nominal performance requirements, turning off the controller will only remove the variable tuning, leaving the nominal tuning intact. Second, the sensitive parts in the system are not placed in the direct path of the fluid flow. This provides the advantage that the debris carried by the fluid in the system will not come in direct contact with the microphone and actuator.

The experimental setup (Figure 3) consists of a Helmholtz resonator cavity connected to the acoustic duct (primary acoustic system) through a short narrow neck. The electrical speaker acting as an actuator is connected to the resonator cavity through an intermediate plate. The speaker is enclosed in an enclosure. A B&K type 4155 microphone acting as a pressure sensor is sealed to the resonator cavity. A monitoring

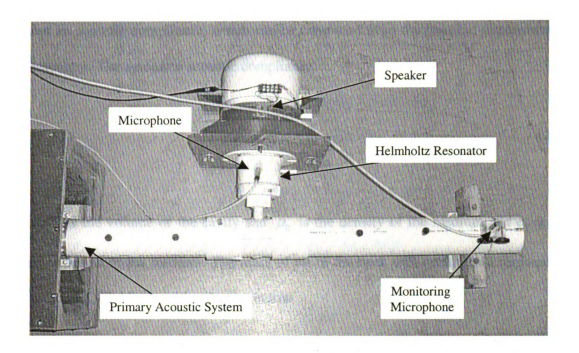


Figure 3 Experimental SHR connected to a primary acoustic system

microphone is connected to the open end of the duct acting as a monitoring device for the performance of the system.

A simple proportional-integral control algorithm is used in the design of the controller for active tuning of the Helmholtz resonator. This controller is first validated using a digital signal processor and implemented using a hybrid controller.

2.2 Analytical Helmholtz Resonator Model

The Helmholtz resonator (Figure 4) is an acoustic device that consists of an enclosed volume and a narrow neck like the shape of a bottle. Temkin (1981) developed a model to obtain the impedance of an acoustic resonator. He studied the action of a monochromatic wave on the device, under the assumption that the lateral dimensions of the cavity were small compared with the wavelength of the incident wave. The cavity

creates an acoustic compliance, which can be computed from the physical dimensions of the resonator. The resonator acoustic compliance

$$C_a = \frac{V}{\rho_o c_o^2},\tag{2.1}$$

where V is the volume of the cavity and ρ_0 is the density of the medium and c_o is the speed of sound in the medium. The mass of air in the neck will oscillate in response to the wave as a solid body with effective inertia

$$I_a = \frac{\rho_o L_e}{S},\tag{2.2}$$

where L_e and S are the effective length and cross sectional area of the neck, respectively. The resonant frequency ω_n of the Helmholtz resonator is a function of the acoustic compliance and the inertia

$$\omega_n = \sqrt{\frac{1}{C_a I_a}} \ . \tag{2.3}$$

The state space representation of the resonator is

$$\frac{d}{dt} \begin{bmatrix} Q_1(t) \\ q_1(t) \end{bmatrix} = \begin{bmatrix} -\frac{R_a}{I_a} & -\frac{1}{C_a I_a} \\ 1 & 0 \end{bmatrix} \begin{bmatrix} Q_1(t) \\ q_1(t) \end{bmatrix} + \begin{bmatrix} \frac{1}{I_a} & 0 \\ 0 & 1 \end{bmatrix} \begin{bmatrix} P_1(t) \\ Q_2(t) \end{bmatrix}, (2.4)$$

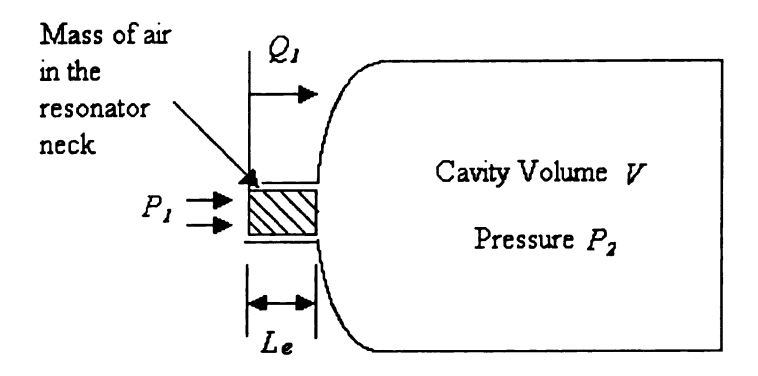


Figure 4 Ideal Helmholtz Resonator

$$\begin{bmatrix} Q_1(t) \\ P_2(t) \end{bmatrix} = \begin{bmatrix} 1 & 0 \\ 0 & \frac{1}{C_a} \end{bmatrix} \begin{bmatrix} Q_1(t) \\ q_1(t) \end{bmatrix}. \tag{2.5}$$

Where the states are: the acoustic volume flow rate through the neck $Q_I(t)$, The volume displacement in the neck $q_I(t)$. The inputs are: $P_I(t)$, the pressure at the neck inlet and $Q_2(t)$, the volume flow rate from the movable surface in the cavity. The outputs are $Q_I(t)$ and The pressure inside the resonator cavity $P_2(t)$ (Birdsong, 1999). The acoustic response of the Helmholtz resonator was obtained by Birdsong (1999). It is defined as the ratio of the volume velocity through the inlet, $Q_I(t)$ (m³/s) to the pressure at the resonator inlet, $P_I(t)$ (N/m²)

$$G_{HR}(s) = \frac{Q_1(s)}{P_1(s)} = \frac{1}{I_a} \left[\frac{s}{s^2 + \frac{R_a}{I_a} s + \frac{1}{C_a I_a}} \right],$$
 (2.6)

where R_a is the dissipation due to radiation losses and viscous damping of the medium.

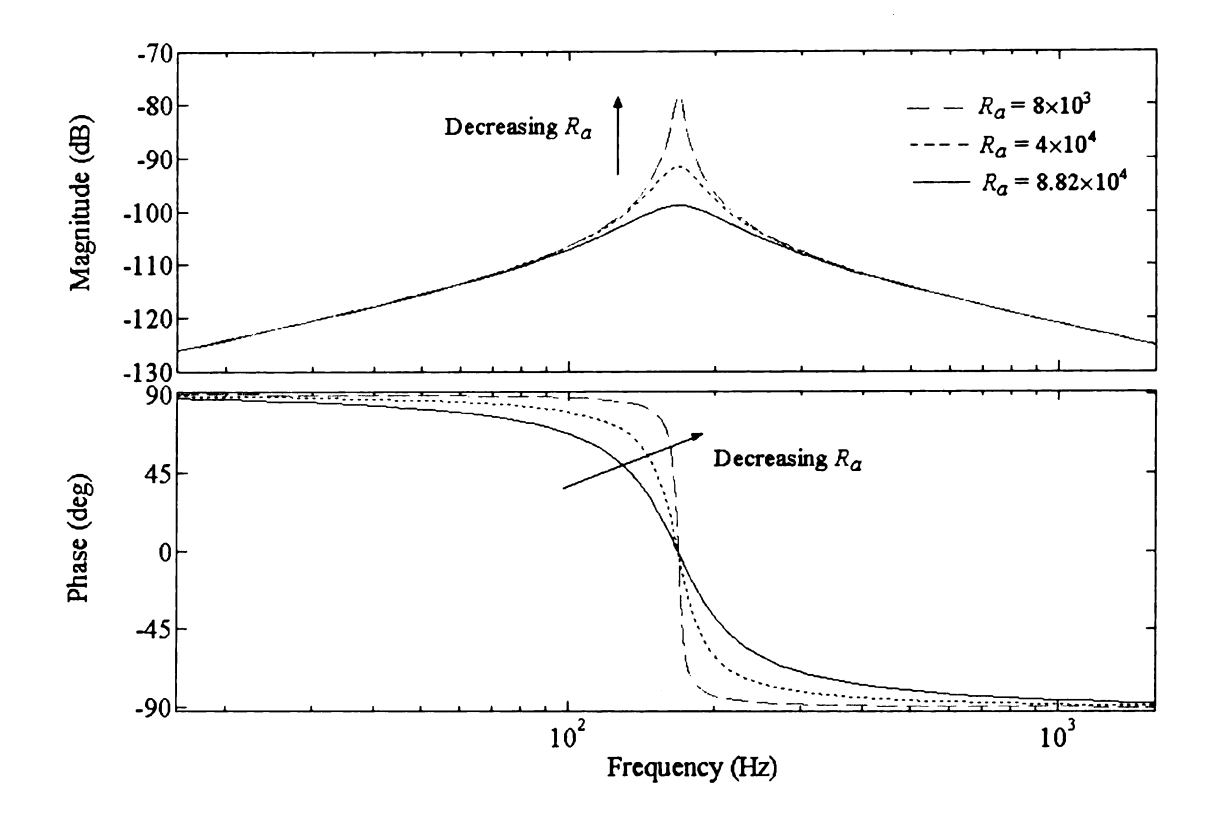


Figure 5 Frequency Response $Q_I(s)/P_I(s)$ of the Helmholtz resonator $(V = 6.71 \times 10^{-4} \text{ m}^3)$, $L_e = 4.00 \text{ cm}$ and $S = 2.54 \times 10^{-4} \text{ m}^2$)

The acoustic frequency response $Q_I(s)/P_I(s)$ of this resonator (Figure 5) has a narrow peak at its resonant frequency and the phase becomes zero at the natural frequency (G_{HR} ($j\omega$) is large and real at the natural frequency). The width of this peak is dependant on the dissipation term R_a . The width of the peak decreases and the magnitude at the resonant frequency increases as the radiation dissipation R_a decreases (Fig 2.4), as expected. Birdsong (1999) described the determination of the radiation loss R_a . The narrow bandwidth and fixed natural frequency limits the conventional Helmholtz resonators to fixed tonal noise suppression. This limitation could be overcome by creating a tunable Helmholtz resonator. Birdsong (1999) achieved this by modifying the interior volume velocity $Q_2(s)$, to the interior pressure $P_2(s)$ response

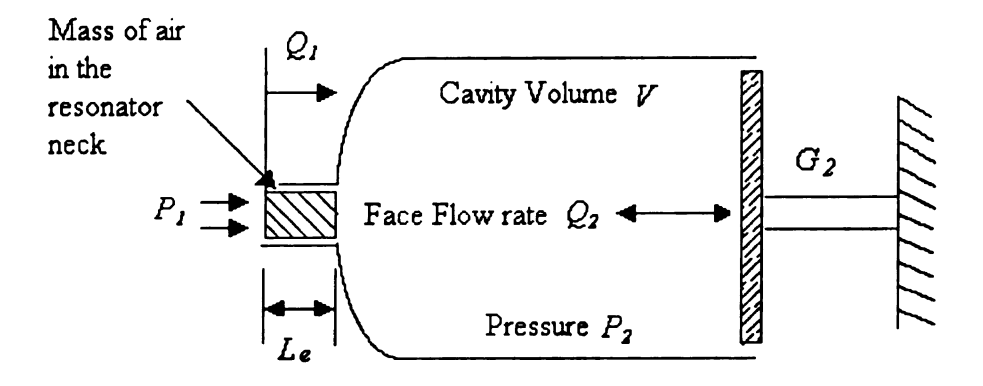


Figure 6 Helmholtz resonator with complex impedance boundary condition

$$G_2(s) = \frac{Q_2(s)}{P_2(s)}. (2.7)$$

The modified semi-active resonator system (Figure 6) functions by generating a volume flow rate from a movable wall in the cavity. This system now has the modified transfer function

$$G_{SHR}(s) = \frac{Q_1(s)}{P_1(s)} = \frac{1}{I_a} \left[\frac{s - \frac{G_2(s)}{C_a}}{s^2 + \left(\frac{R_a}{I_a} - \frac{G_2(s)}{C_a}\right)s + \frac{1}{C_aI_a} (1 - R_aG_2(s))} \right]. \tag{2.8}$$

modifying boundary surface response $G_2(s)$ modifies the resonant frequency. Birdsong (1999) proposed the use of a simple Proportional-Integral controller

$$G_2(s) = \frac{Q_2(s)}{P_2(s)} = K_p + \frac{K_i}{s}.$$
 (2.9)

The closed loop transfer function in terms of controller gains K_p and K_i with negative feedback can be obtained by substituting (2.9) in (2.8) as

$$\frac{Q_1(s)}{P_1(s)} = \frac{1}{I_a} \left[\frac{s^2 - \frac{1}{C_a} \left(K_p + \frac{K_i}{s} \right) s}{s^3 + \left(\frac{R_a}{I_a} - \frac{K_p}{C_a} \right) s^2 + \left(\frac{1}{C_a I_a} - \frac{K_i}{C_a} - \frac{R_a K_p}{I_a C_a} \right) s - \frac{R_a K_i}{I_a C_a}} \right].$$
(2.10)

Changing the controller gains K_p and K_i changes the dynamic response of the system. The necessary and sufficient conditions for this system to be stable are

$$K_i < 0, \tag{2.11}$$

$$K_p < \frac{R_a C_a}{I_a},\tag{2.12}$$

$$K_{p} < \left[\frac{1}{R_{a}} - \frac{K_{i}I_{a}}{R_{a}} \right]. \tag{2.13}$$

These bounds on the gains determine the limitation of the controller to tune the system, defining a design space for the controller gains. The root locus for K_p (Figure 7(a)) with $K_i = 0$ shows that K_p predominantly changes the damping. A similar root locus for K_i (Figure 7(b)) with $K_p = 0$ shows that K_i predominantly changes the resonant frequency. The direction of arrow in the root locus (Figure 7) represents the direction of increasing negative parameter. The model shows $K_i < 0$ for closed loop stability. The positive limit on K_p defines the maximum amount of damping that can be removed before marginal stability could be reached and the limit on K_i defines the directional movement of the resonant frequency from the nominal value. This indicates that by varying the controller gains, the resonant frequency and damping could be varied. The above analysis motivated

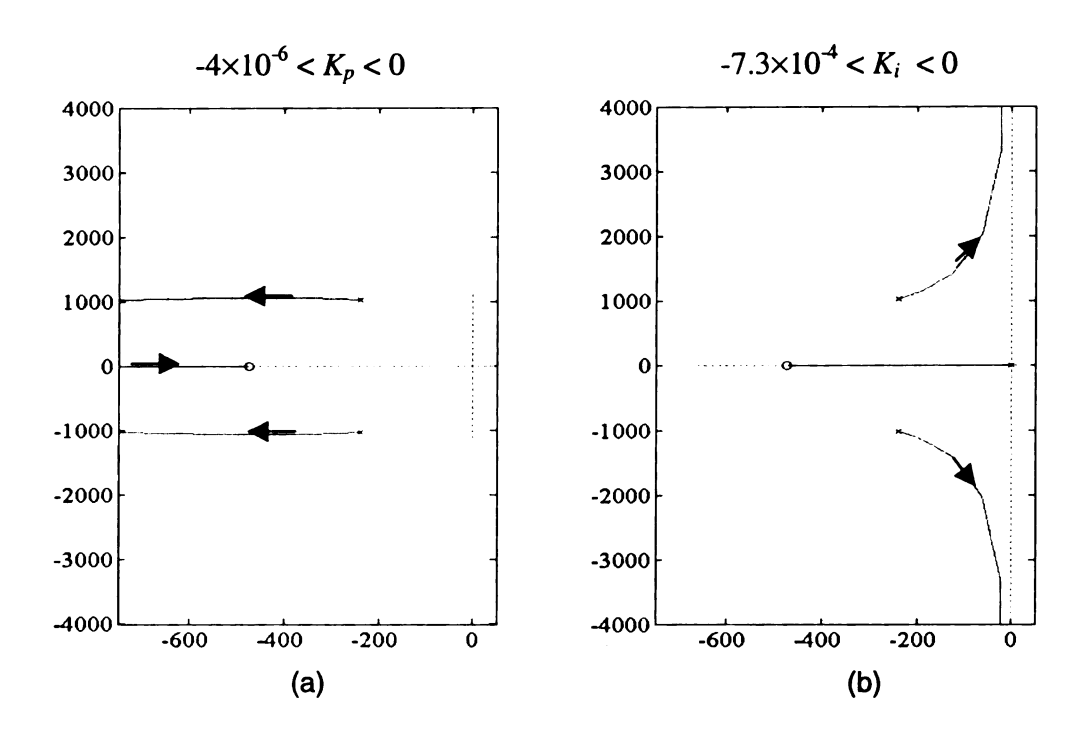


Figure 7 Complimentary Root locus for (a) K_p with $K_i = 0$ (b) K_i with $K_p = 0$

the use of a PI controller in retuning the resonant frequency of the Helmholtz resonator. The advantage of this method is that the response of the resonator can be changed without changing the physical dimensions of the resonator. All the above analysis was based on the assumption that the actuator is not associated with any dynamics.

2.3 Actuator and its effect on SHR

The actuator is a critical component in the implementation of the transfer function (2.8). Electromechanical actuators like audio speakers could be used as acoustic actuators to generate the required interior volume velocity $Q_2(t)$. An electromechanical speaker is chosen as an actuator because of their simplicity, low cost and availability. Speakers are not ideal actuators but have dynamic characteristics. Birdsong (1999) discussed the

dynamic modeling of the speaker and its effect on the performance of the SHR in detail.

The state space representation of the actuator model is

$$\frac{d}{dt} \begin{bmatrix} Q_{2}(t) \\ q_{2}(t) \\ \lambda(t) \end{bmatrix} = \begin{bmatrix} \frac{-R_{s}}{I_{s}} & \frac{-1}{C_{s}I_{s}} & \frac{blS_{d}}{I_{c}I_{s}} \\ 1 & 0 & 0 \\ \frac{-bl}{S_{d}} & 0 & \frac{-R_{m}-R_{c}}{I_{c}} \end{bmatrix} \begin{bmatrix} Q_{2}(t) \\ q_{2}(t) \\ \lambda(t) \end{bmatrix} + \begin{bmatrix} 0 & \frac{-S_{d}^{2}}{I_{s}} \\ 0 & 1 \\ 1 & 0 \end{bmatrix} \begin{bmatrix} e_{p}(t) \\ P_{2}(t) \end{bmatrix}$$
(2.14)

$$\begin{bmatrix} i_{p}(t) \\ Q_{2}(t) \end{bmatrix} = \begin{bmatrix} 0 & 0 & \frac{1}{I_{c}} \\ 1 & 0 & 0 \end{bmatrix} \begin{bmatrix} Q_{2}(t) \\ q_{2}(t) \\ \lambda(t) \end{bmatrix}$$
(2.15)

where the states are the volume velocity of the speaker face $Q_2(t)$, volume displacement of the speaker face $q_2(t)$ and the magnetic flux in the speaker coil $\lambda(t)$. The inputs are: primary coil voltage $e_p(t)$ and pressure on the speaker face $P_2(t)$. The outputs the primary coil current, $i_p(t)$ and the speaker volume velocity $Q_2(t)$.

The different speaker parameters that are involved in the model are the speaker face area S_d , speaker inertia I_s , speaker compliance C_s , speaker friction R_s , speaker coil resistance R_c , speaker coil inductance I_c , speaker electromechanical coupling factor bl, and the primary coil current sensing resistance R_m . The parameters associated with the dynamic model of the speaker were identified and tabulated in Table 11 using the method specified by Radcliffe and Gogate (1995).

Table 1 Analytical model parameter values

C_0	343 m/s	I_c	2.26 mH
$ ho_0$	1.18 Kg/m ³	M_c	1.4 mH
V	$6.71 \times 10^{-4} \text{ m}^3$	Smic	40 mV/Pa
Le	4.80 cm	S	2.54×10 ⁻⁴ m ²
C_a	4.83×10 ⁻⁹ m ⁵ /N	S_d	1.33×10 ⁻² m ²
I_a	222 Ns ² /m ⁵	R_c	7.86 Ω
R_a	8.82×10 ⁴ Ns/m ⁵	R_m	0 Ω
C_s	6.21 ×10 ⁻⁴ m/N	bl	2.45 N/A
Is	4.1×10 ⁻³ Kg	R_s	1.6007 Ns/m

2.4 Controller design with actuator dynamics

Actuator dynamics adds additional complexity to the controller design. The effect of actuator dynamics on the controller design can be determined by examining the closed loop pole locations. The addition of the actuator model to the SHR adds additional dynamics and therefore there are more poles. The Helmholtz resonator is a second order model, the controller is a first order model and the actuator is a third order model. Hence the combination is a sixth order model. It is difficult to find a solution for the sixth order model that maps the controller gains K_p and K_i to ω_h and ξ . There is no closed form solution to find the gains as a function of desired closed loop eigenvalues. A model based trial and error technique was used to determine the controller gains. A good starting point was the gains found in the analytical controller design without actuator dynamics. As before, the integral gain primarily changes the apparent natural frequency and the proportional gain primarily changes the damping.

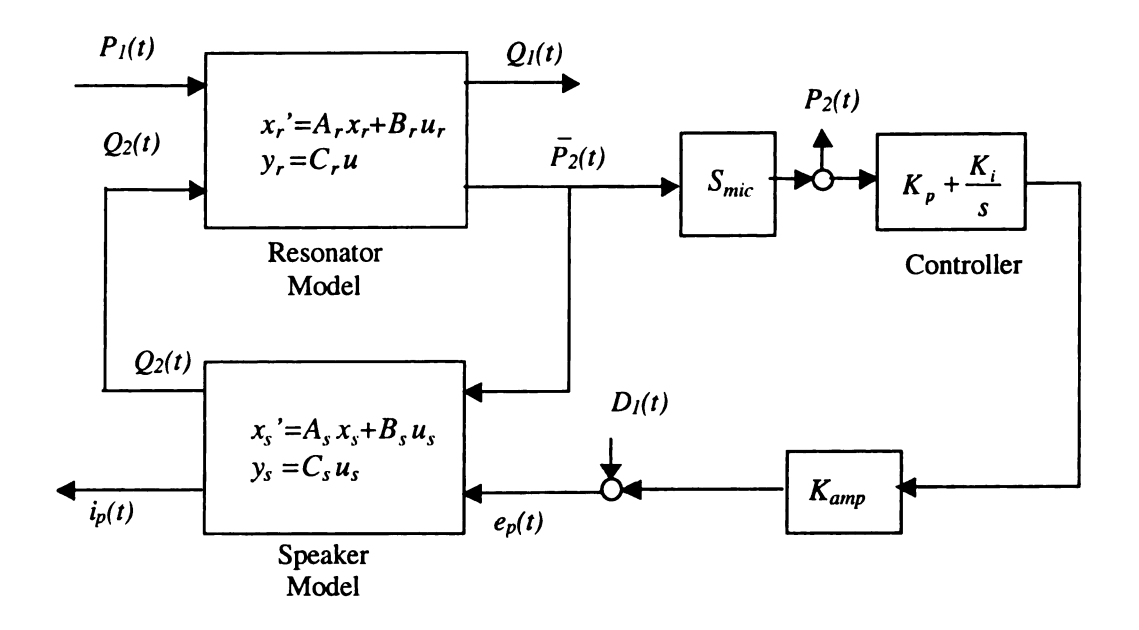


Figure 8 Closed loop coupled model of the SHR

The closed loop system (Figure 8) consists of a resonator model, speaker model, controller model and the gains associated with the microphone (S_{mic}) and the power amplifier (K_{amp}). The pressure $P_2(t)$ sensed in the resonator cavity is converted into an equivalent voltage (S_{mic}) and this pressure is given as an input to the controller. This controller implements the PI control action and drives the speaker through a power amplifier (K_{amp}).

An analytical controller design was developed by computing an analytical mapping from the controller gains to the resonant frequency, ω_n , and damping, ξ , of the closed loop system (Birdsong, 1999). In order to measure the system response, a disturbance signal $D_I(t)$ was injected analytically to the coil of the actuator. This input was applied to be consistent with the planned experimental tests. The frequency response for the transfer function $P_2(s)/D_I(s)$ for the resonator, speaker and the feedback controller

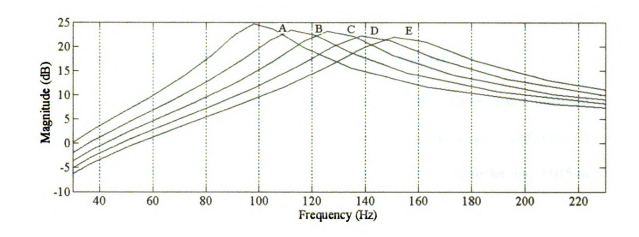


Figure 9 Simulated frequency response of the transfer function P₂(s)/D_f(s) for the SHR with α_k=100Hz, 114Hz, 127Hz, 140Hz and 153Hz.

Table 2 Controller gains for $K_{amp} = 1$, $\xi = 0.10$ and $S_{mic} = 0.04$

Curve	Α	В	C	D	Е
Resonant Frequency (Hz)	100	114	127	140	153
K_p	1.08	1.07	1.05	1.03	1.01
K_i	-100	-150	-200	-250	-350

model was computed (Figure 9) for different values of K_p and K_i (Table 2). From the Table 2.2, it can be observed that the resonant frequency changes by 50% for a 7% change in value of K_p a 250% change in value of K_i . These behaviors show that the damping, ξ is very sensitive to small changes in K_p . Change in K_p produces a change in the damping and a change in K_i produced a change in the resonant frequency as predicted by the model. The model based trial and error controller design produces a mapping between the controller gains and the resonant frequency and damping. Due to the sensitivity in the values of K_p , the model requires an experimental validation.

2.5 Experimental Model Validation with DSP Board

The experimental set up (Figure 3) consisted of the Helmholtz resonator, enclosed acoustic actuator, acoustic duct, disturbance speaker, microphone and controller. A cylindrical Helmholtz resonator cavity with dimensions 0.075 m in diameter and 0.015 m in length is used with a cylindrical neck with dimensions 0.018 m in diameter and 0.04 m in length glued to one end of the cavity. The control system consisted of a half inch B&K type 4155 microphone sealed through the wall of the cavity as shown in Figure 3. As a preliminary experiment before developing the hybrid circuit, A Dspace Model #1102 floating point, digital signal processor was used to implement the controller. A 6 inch dual voice coil speaker was used as an actuator. A dynamic signal analyzer (HP35660A) was used to measure the frequency response.

In all phases of the design, the system was separated from any primary acoustic system. The usefulness of the device would be limited if the SHR response was dependant on the structure of the primary acoustic system. Resonators can be designed with a tuning frequency and then applied to any primary system to attenuate noise at that frequency.

The schematic of the experimental set up (Figure 10) shows that the pressure signal from the resonator cavity is sent into the digital signal processor. The digital signal processor implements the control action and drives the speaker through an amplifier.

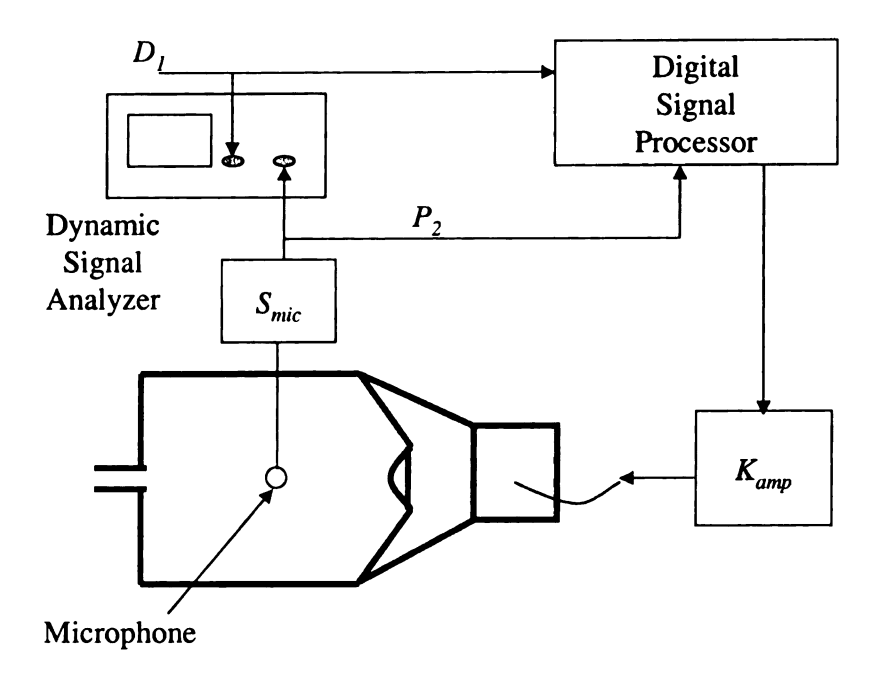


Figure 10 Experimental setup using the digital signal processor

The PI controller design was based on quantitative information learned from the model. The objective was to find the gains K_p and K_i , that placed the resonance at various frequencies, while maintaining stability. The data was collected by fixing K_i , searching for K_p that produced desired peak amplitude and recording the resonant frequency. In order to measure the system response, a disturbance signal $D_I(t)$ was injected through the secondary coil of the speaker. This was done because, it was difficult to measure the quantities $Q_I(t)$ and $Q_2(t)$. The model was validated by looking at the response of $P_2(s)/D_I(s)$. The gains K_p and K_i obtained from the response are plotted against resonant frequency (Figure 11), which compares the experimentally derived controller gains with the model derived controller gains. Note that although there is a difference in the magnitude of K_p and the initial values of K_i , the overall trend of these graphs agree. The difference in the K_p is attributed to the difficulty in estimating the damping parameters in

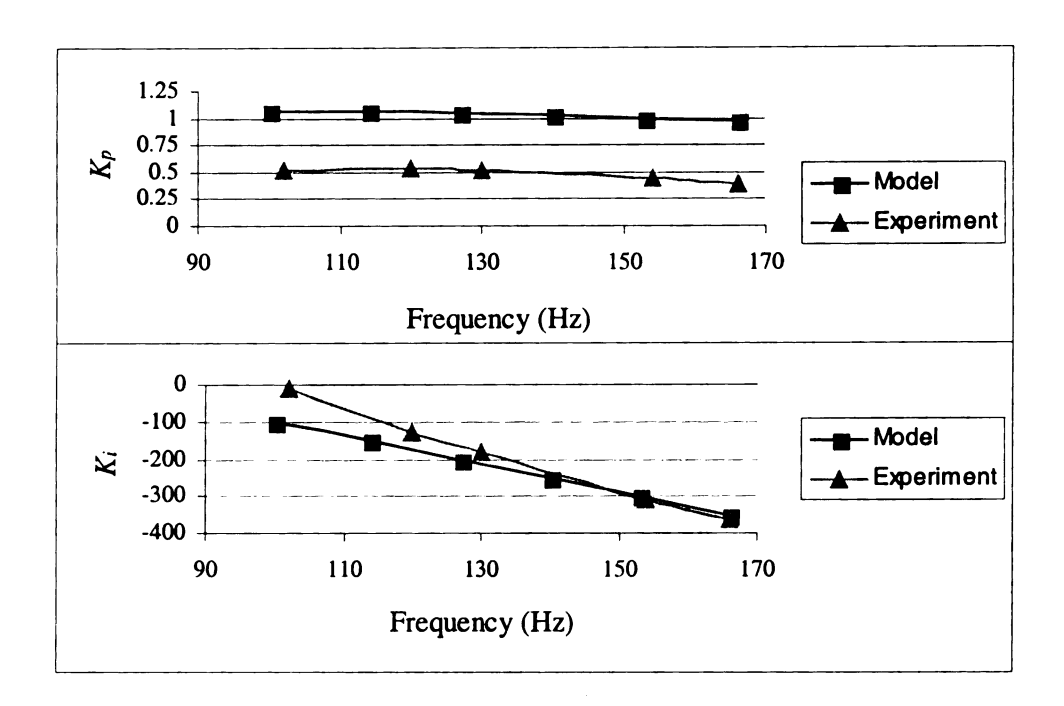


Figure 11 Comparison of K_p and K_i Vs ω_n

the model. The experiment allowed fine-tuning of gains especially K_p associated with damping.

The tuning capabilities of the device are illustrated by the closed loop frequency response measurements. A disturbance $D_I(t)$ was injected through the secondary coil of the speaker in the absence of any primary disturbance $P_I(t)$. The frequency response $P_2(s)/D_I(s)$ (Figure 12) was measured for 4 different experiments. The curves A, B, C and D show the resonant peak for separate experiments with $\omega_n = 100$, 126,137 and 164 Hz. For each experiment, the controller gains were changed manually.

The experimental frequency response of $P_2(s)/D_1(s)$ (Figure 12) illustrates that the resonant frequency of the Helmholtz resonator could be modified by changing the

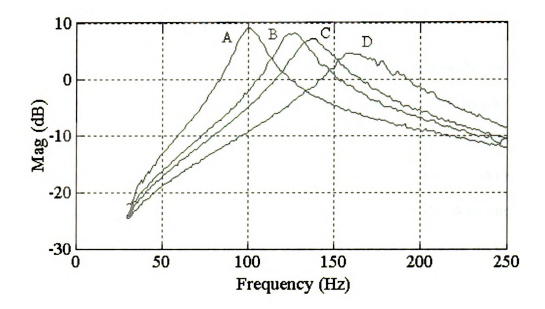


Figure 12 Experimental frequency response $P_2(s)/D_1(s)$ for gain scheduling controller using the Dspace board with $\omega_n = 100$, 126, 137 and 164 Hz

controller gains as predicted by the model. The result demonstrates the ability of the controller to tune the SHR to arbitrary frequencies. The adaptation of the SHR for different frequencies of excitation was achieved manually.

These experimental results demonstrated that a self-tuning microcontroller was needed with the same characteristic behavior as the Dspace controller board but with the added advantage of a self-tuning algorithm. The experimentally determined values of the controller gains were used for the gain scheduling algorithm and self-tuning.

3 Hybrid Controller

The hybrid controller includes both analog and digital subsystems to optimize itself over a wide range of operating conditions. The digital controller section uses controller input, output, and auxiliary inputs to optimize the performance of analog portion of the controller. As operating conditions change, purely analog systems are difficult to reconfigure for optimal conditions. A hybrid controller developed here is more economical than using an analog interface board in a computer to realize the control algorithm.

3.1 Hybrid control system

The Hybrid controller (Figure 13 (a)) consists of an analog circuit, comparator and a microcontroller. The resonator cavity pressure P_2 acts as an input to both the comparator and the analog circuit. The analog circuit implements the PI control action. Since the disturbance signal is a sinusoidal wave, the pressure P_2 also has a sinusoidal behavior of the same frequency. When this pressure signal passes through the comparator circuit, it is converted into a square wave of the same frequency. This square wave acts as an input to the microcontroller. The microcontroller measures the incoming frequency and selects the corresponding controller gains K_p and K_i . These control gains are set on the analog portion of the circuit. The analog circuit outputs a voltage e_p to drive the speaker through an amplifier. The microcontroller is preprogrammed to make it self-tuning. The experimental hybrid controller (Figure 13 (b)) was built using operational amplifiers, digital potentiometers and a Basic StampTM microcontroller.

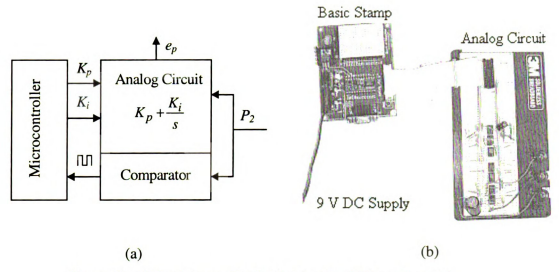


Figure 13 Hybrid Controller (a) Schematic (b) Experimental

3.2 Analog Circuit

Analytical model of the analog circuit is necessary in order to compare the magnitude and phase of the experimental signal with the analytical model at each stage. The cavity pressure P_2 and the required actuator velocity Q_2 are expressed in terms of equivalent voltage. The required controller transfer function (2.9) is modified to

$$\frac{V_o}{V_i} = \frac{Q_2}{P_2} = K_p + \frac{K_i}{s + p_1} \tag{3.1}$$

to eliminate the infinite gain associated with the integral control at very low frequencies. A pole is added at a very low frequency compared to the required frequency band by adding a resistor R_8 parallel to the capacitor C_2 (Figure 14). V_o denotes the output voltage of the analog circuit equivalent to the required actuation velocity Q_2 and V_1 denotes the measured cavity pressure P_2 in terms of equivalent voltage. Multiple stages have been

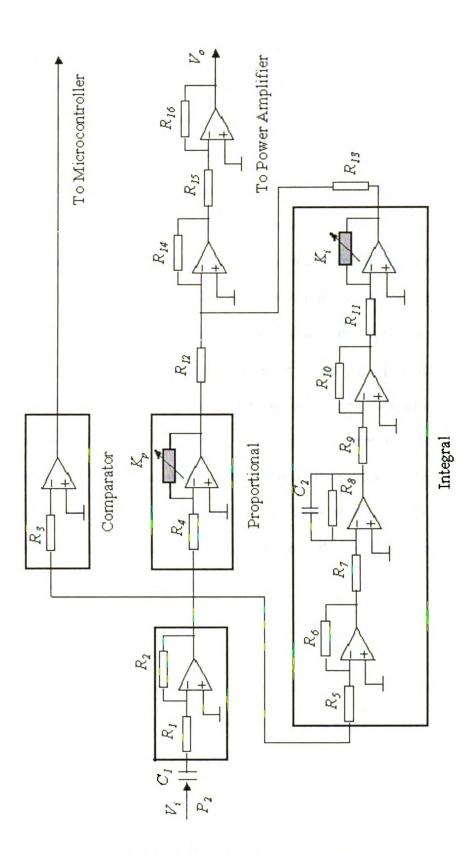


Figure 14 The complete analog circuit

used to achieve the desired gains. The input to the circuit from the microcontroller is only a steady 5 V supply. Hence single supply operational amplifiers of type LM358N were used in the design of the analog circuit. The reference level of the circuit is changed from the ground state, 0 V to the midrange value 2.5 V. This is achieved by a simple voltage divider circuit. The reference voltage generated by the potential divider is connected to the positive terminals of all the single supply operational amplifiers in order to keep the signal within the common range of the devices. An input coupling capacitor, C_l , is added to the circuit in order to eliminate the DC component at the input. The capacitor value is chosen in such a way that the dynamics associated with this capacitor has negligible effect on the system. The control gains could be varied by replacing the feedback resistors of the fixed gain amplifiers with potentiometers K_p and K_i (Figure 14). A further improvement is achieved by replacing these analog potentiometers with digital potentiometers (DS1804) so that digital manipulation of the gains could be achieved with the use of the Basic StampTM microcontroller. The values of the resistors and capacitors are listed in Appendix A. The magnitude and phase of the signal was verified with the theoretical model at each stage.

3.3 Microcontroller

Basic StampTM micro-controller is used to implement the digital controls to the analog circuit. The use of a microcontroller allows analog signals, detected by a sensor, to be digitized for further hardware manipulation. This is done in accordance with the software programmed into the Basic StampTM. The Basic StampTM is an inexpensive microcontroller with a built-in BASIC interpreter. The hardware consists of a PBASIC interpreter chip (PIC), Program memory, Programming connection, Power supply, Reset

circuit and 16 I/O pins. Writing programs for the Basic Stamp[™] is accomplished with a special version of the basic language called PBASIC. This Basic Stamp[™] executes about 4000 BASIC instructions per second. The direction, input or output, of a given I/O pin is under the control of the BASIC program. These basic instructions are interpreted by the PIC. Since the PIC's internal memory is occupied by the language, the program is stored in an EPROM. Whenever the battery is connected, stamps run the basic program in memory. Stamps can be reprogrammed at anytime by temporarily connecting them to a PC running a simple host program. This is achieved by the programming connection. The voltage regulator on the Basic Stamp[™] takes an input voltage from 6 to 15 Volts and converts it to 5 Volts that the stamps require.

3.4 Frequency estimation and self-tuning

Accurate frequency estimation is required in order to implement the self-tuning capability effectively using the gain scheduling algorithm. In order to have better frequency estimation, a comparator is added to the analog circuit. Since the input disturbance is a pure tonal noise, the output of the comparator becomes square wave. This resulting square wave was sent to one of the pins of the Basic StampTM microcontroller as input. The command in the Basic StampTM computes the period of the square wave. For real time average frequency measurement, a simple IIR filter algorithm was implemented. The real time average reduces variation in computed frequency. The desired gains were obtained from the lookup table provided in the Basic StampTM program. These values were used to manipulate the digital potentiometers, K_p and K_i . (Figure 14) in order to achieve the control algorithm. The controller gains obtained experimentally (section 2.5) were used to design the set points on the digital potentiometers for various frequencies.

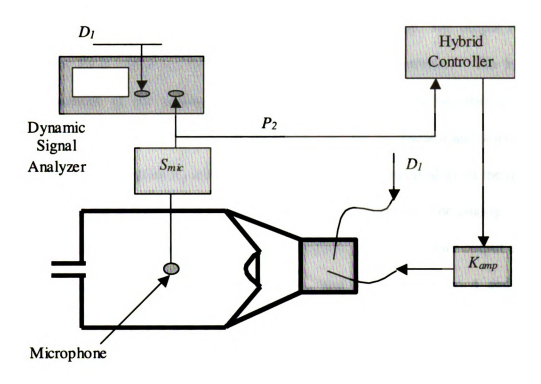


Figure 15 Schematic of the experimental setup using microcontroller

These set points were tabulated with the corresponding frequencies as shown in Appendix A. The algorithm and program used for the Microcontroller is shown in Appendix B.

3.5 Experimental Results

The experimental setup consisted of the SHR described in section 2.5. The Dspace board is replaced by the Hybrid controller. The hybrid controller consisted of an analog circuit with LM358N operational amplifiers, DS1804 digital potentiometers and a Basic Stamp[™] microcontroller. The SHR is connected to an acoustic duct (Figure 15). An additional B&K type 4155 half-inch microphone was used to monitor the performance of the device at the open end of the duct (P₃(t)).

The schematic (Figure 15) illustrates the experimental setup. The output of the pressure sensor P_2 is connected to the input of the hybrid PI controller. The hybrid controller consisted of the analog circuit, comparator and the microcontroller. The microcontroller estimates the frequency of the signal from the comparator and selects the corresponding controller gains K_p and K_i . These controller gains are used to set the digital potentiometers in the analog circuit to their corresponding set points. The analog circuit achieves the desired control action for a particular frequency. The controller output drives the speaker through an amplifier. The gains K_{amp} and S_{mic} were set to 4 and 0.01 respectively.

The experimental frequency response (Figure 16) of the transfer function $P_2(s)/D_1(s)$ was measured for 5 experiments, curves labeled A, B, C, D and E, using the controller gains in Table 3. The gains were able to shift the resonant frequency from 100 Hz to 178 Hz. As predicted by the model, the hybrid controller was able to amplify the resonant peak and shift the resonant frequency. As the integral gain was increased, the system moved close to the unstable region and hence the damping was increased by modifying the proportional gain.

In the next experiment, the resonator was connected to an acoustic duct with a disturbance speaker at one end. A pure tonal noise was injected through the disturbance speaker. The resonator cavity pressure $P_2(t)$ and the open duct pressure $P_3(t)$ were measured using half inch B&K type 4155 microphones. With an open loop system, the sound pressure level measured was 112 dB at 132 Hz (Figure 17). With the closed loop system, the sound pressure level measured was 92 dB. This represents a 20 dB noise

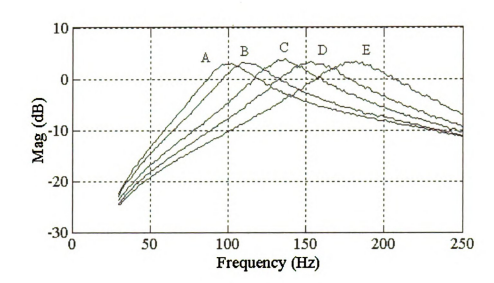


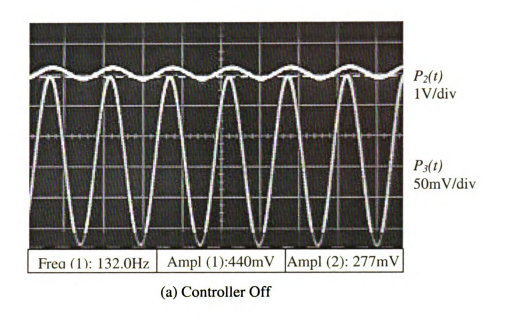
Figure 16 Experimental frequency response $P_X(s)/D_I(s)$ for gain scheduling controller with ω_n = 100, 112, 135, 154 and 178 Hz and with gains set to zero

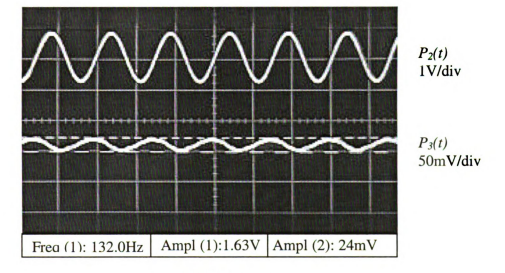
Table 3 Controller gains for analog circuit

Curve	A	В	C	D	E
Resonant Frequency (Hz)	100	112	135	154	178
K_p	0.52	0.52	0.51	0.43	0.35
K_i	0	-80	-210	-310	-430

reduction. The same experiment was conducted at a disturbance frequency of 147 Hz (Figure 18). The sound pressure level measured with the controller off at the open end of the duct was 108 dB. When the controller was turned on, the sound pressure level dropped to 90 dB representing a reduction of 18 dB. Similar experiments were performed for different frequencies and it was observed that the noise reduction maintained at approximately 20 dB for frequencies ranging from 123 Hz to 153 Hz. The noise reduction dropped to 12 dB at 100 Hz and 10 dB at 163 Hz. At higher frequencies,

the amplifier gains were restricted due to the saturation of the operational amplifiers. It was also observed that the pressure in the resonator cavity increased by approximately 4 times as expected when the controller was switched on. This represents that the resonator is at its resonance when the controller was switched on. The self-tuning algorithm explained in the previous section was implemented by programming the Basic StampTM microcontroller and tested on the circuit. The hybrid controller was able to track the frequency of the disturbance signal and attenuate the noise with frequencies ranging between 100 Hz and 163 Hz.





(b) Controller on

Figure 17 Experimental Sound pressure measured in the resonator cavity (top channel) and the output of the acoustic duct (bottom channel) at 132 Hz (a) with controller off (b) with controller on

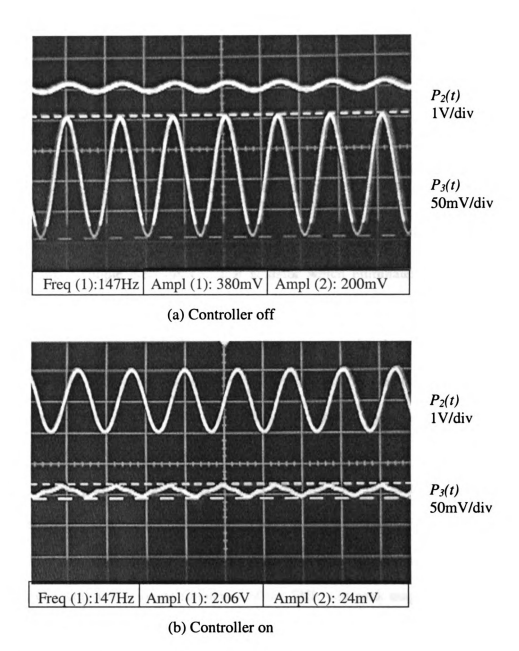


Figure 18 Experimental Sound pressure measured in the resonator cavity (top channel) and the output of the acoustic duct (bottom channel) at 147 Hz (a) with controller off (b) with controller on

4 Conclusions

This work presents a method for designing a self-tuning semi active Helmholtz resonator. This device is designed independent of the primary acoustic system. No sensors are required external to the device, so that its operation is not dependant on the structure of the primary acoustic system. The device could be attached to any system generating a time varying frequency signal. The acoustic impedance of the system is modified by using a simple electromechanical actuator which eliminates the complex mechanical moving structures. The sensitive components such as sensors are placed safely in the resonator cavity which eliminates their exposure to harsh environments. In the event of controller failure, the resonator provides nominal noise reduction. A simple Proportional-Integral controller is used to modify the system dynamics within the stability region. The controller gains were obtained by using model based trial and error techniques. A simple gain scheduling algorithm is developed for the self-tuning of the device. The self-tuning is achieved with a simple digital-analog circuit integrated with a Basic StampTM microcontroller. The device has the advantage of tracking disturbance frequency and changing the resonant frequency of the SHR and peak magnitude online. The only power requirement for the hybrid controller is a 9 V DC supply. Noise reduction of approximately 10 - 20 dB was achieved within a narrow band of frequencies ranging from 100 Hz to 163 Hz. This hybrid controller is very economical and compact.

Bibliography

Bedout, Francheck, et. Al. 1997, "Adaptive-Passive Noise Control with Self-Tuning Helmholtz Resonators," Journal of Sound and Vibration, 202, p109-123

Benjamin, C. Kuo., 1997, Automatic Control Systems, Seventh Edition, Prentice-Hall Inc.

Bernhard, R.J., Hall H.R. and Jones J.D., 1992, "Adaptive-Passive Noise Control," Inter-Noise 92.

Birdsong, C., 1999, "A Semi-Active Helmholtz Resonator," PhD Dissertation, Michigan State University, East Lansing, Michigan.

Koopman, G. and Neise, W., 1982, "The use of Resonators to silence centrifugal blowers," Journal of Sound and Vibration, 82, p17-27.

Lamancusa, J.S., 1987, "An Actively Tuned Passive Muffler System For Engine Silencing," Proceedings of Noise-Con 87, p313-318

Nelson, P.A. and Elliot S.J., 1992, Active Control of Sound, Academic Press

Parallax Inc., 1998, Basic Stamp Manual, Version 1.9

Phillips, C.L. and Harbor, R.D., 2000, Feedback Control Systems, Fourth Edition, Prentice-Hall Inc, New Jersey

Pierce, Allan D., 1981, Acoustics: An Introduction to its Physical Principles and Applications, McGraw-Hill Book Co, New York

Radcliffe, C.J and Birdsong, C., 2001, "An Electronically Tunable Resonator for Noise Control," 2001-01-1615, Society of Automotive Engineers.

Radcliffe, C.J. and Birdsong, C., 1998, Hybrid Digital-Analog Controller, Michigan State University Intellectual Property Disclosure, No 98-049.

Radcliffe, C.J. and Gogate, S.D., 1995, "Development of an Active Acoustic Sink For Noise Control in Acoustic Spaces," PhD Dissertation, Michigan State University, East Lansing, Michigan

Temkin, 1981, Elements of Acoustics, John Wiley & Sons Inc

Tokhi, M.O and Leitch, R.R., 1992, Active Noise Control, Oxford Science Publications.

Appendix

Appendix A

Table 4 Analog Circuit component values

R_I	10	R ₁₀	10
R_2	1	R_{II}	10
<i>R</i> ₃	1	R_{12}	1
R ₄	10	R ₁₃	1
R ₅	1	R ₁₄	1
R ₆	2	R ₁₅	1
R ₇	1	R ₁₆	1
R_8	5	C_{I}	3300
R ₉	1	C ₂	22

All resistor values are mentioned in k Ω s, and capacitor values are in μF .

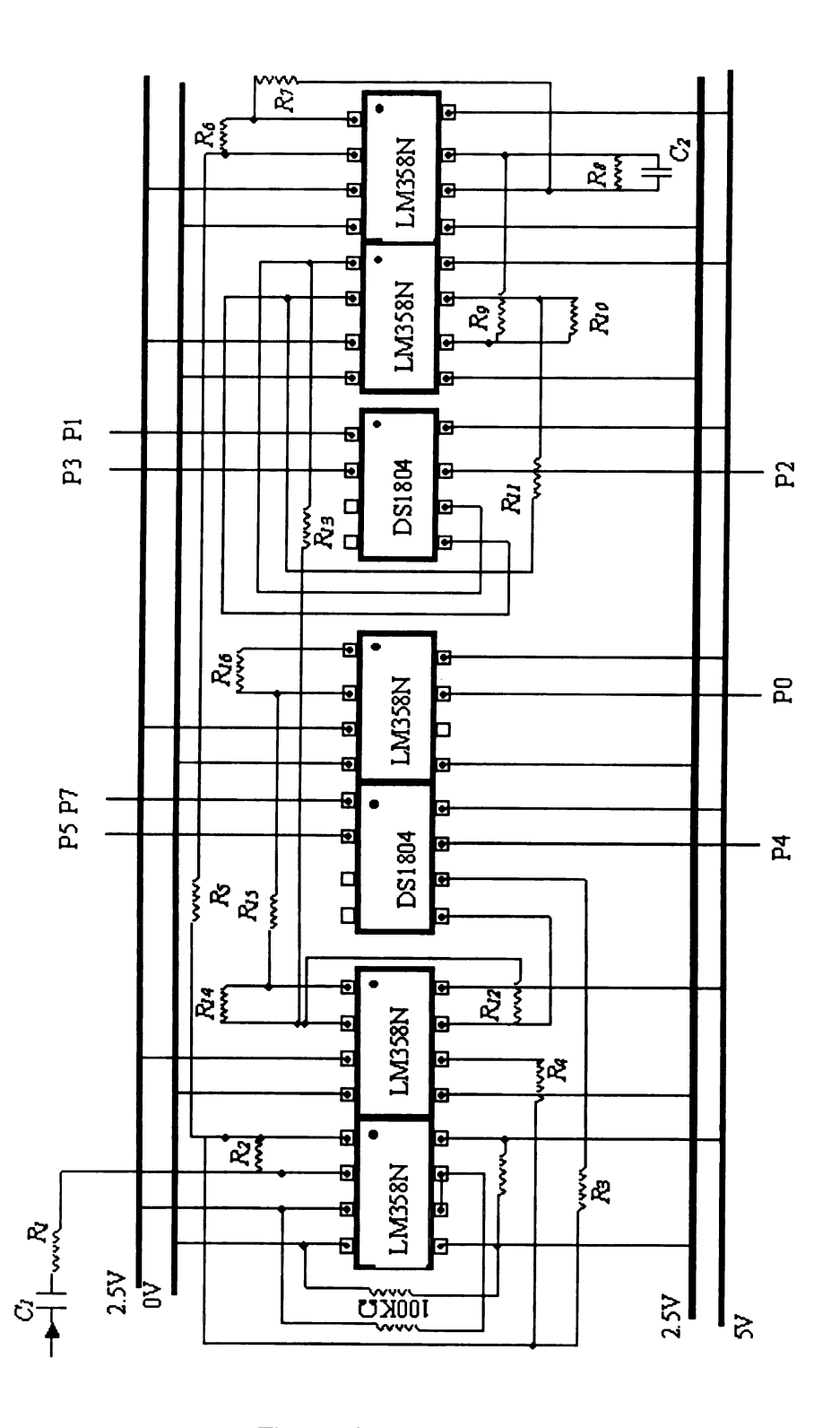


Figure 19 Analog Circuit

Appendix B

Algorithm used for programming Basic StampTM

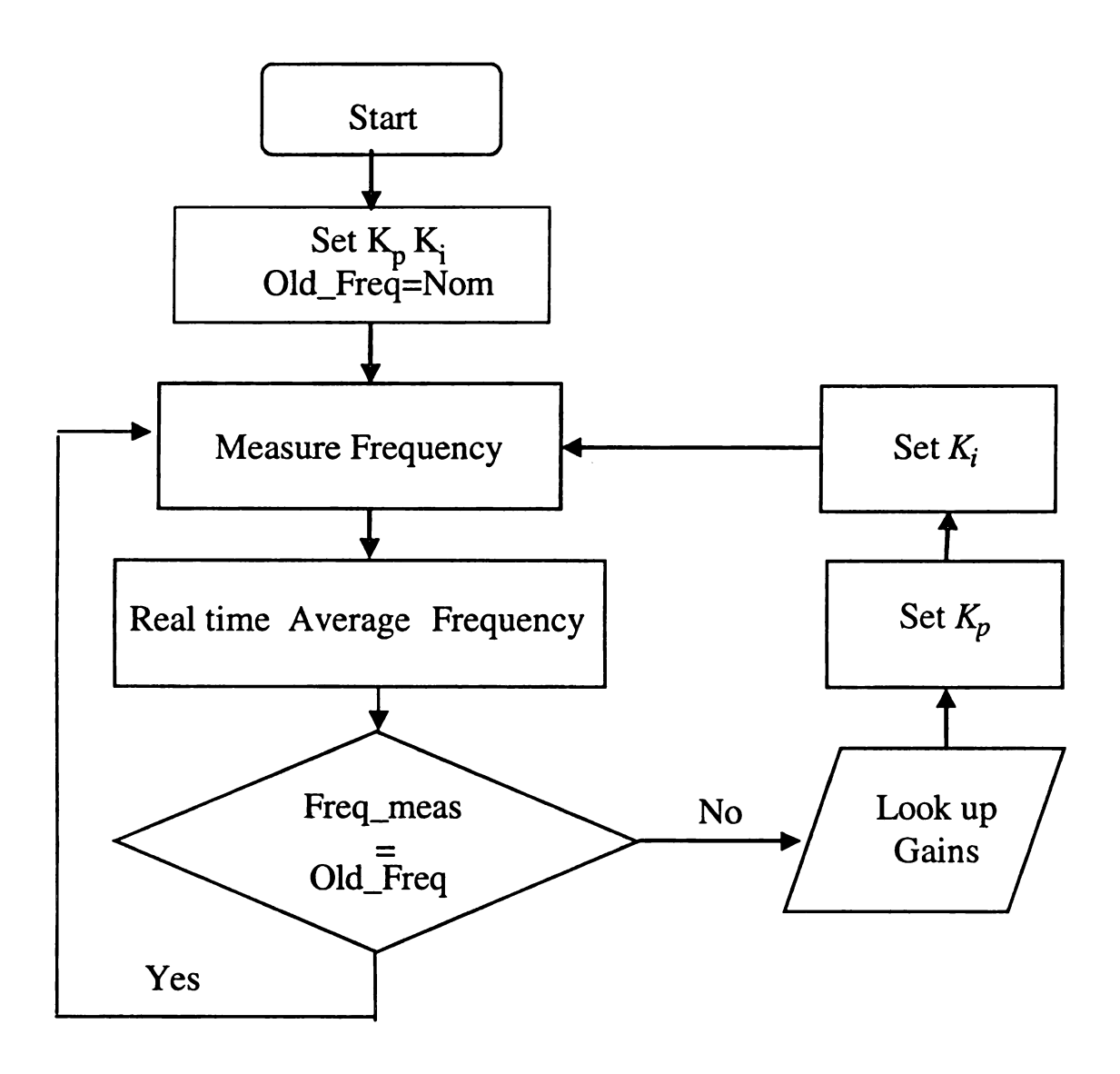


Figure 20 Self-Tuning Algorithm

Program for the Basic StampTM microcontroller for self-tuning

'{\$STAMP BS2}

'Control gains are set through these constants

Kp	var	word	'Kp gain in kOhms
Ki	var	word	'Ki gain in kOhms
Kp_inc	var	word	'Get Kp to the set value
Ki_inc	var	word	'Get Ki to the set value
Kp_old	var	word	'Store the old Kp
Ki_old	var	word	'Store the old Ki
pulsew	con	125	'control pulse width in 2 us increments
pin	con	2	'Pin for measuring frequency

'Kp digital resistor control line connections

KpSelect con 4 'Kp chip select

KpUpDn con 5 'Kp up-down control (up=high, down=low)
KpInc con 7 'Kp increment control (one pulse per step)

'Ki digital resistor control line connections Ki Select con 0 'Ki digital resistor chip select line

KiSelect	con 0	'Ki digital	resistor chip select line
KiUpDn		con 1	'Kp up-down control (up=high, down=low)
KiInc		con 3	'Kp increment control (one pulse per step)

X	var	word	'Used in pot up/down and rounding
freq	var	word	'Input frequency
avg	var	word	'Running cumulative
index	var	word	'Look up variable (or) frequency
avg_freq var	word	'Running a	verage frequency
avg_freq_old	var	word	'Old frequency
freq_roundvar	word	'Used for f	frequency rounding

'Initialize values

avg_freq=0 Kp=0 Ki=0

freq_round=0

'Initialize Control lines

output KpSelect output KpUpDn output KpInc output KiSelect output KiUpDn output KiInc

Initialize	Proportional Control			
ow KpInc 'initialize increment control line				
low KpSelect	ct 'select chip			
'reset the proportional resistor to	0 0			
low KpUpDn	KpUpDn 'increment resistance down to initialize x = 1 to 99 'resistor has 99 steps numbered 0-99			
for $x = 1$ to 99				
pulsout KpInc, pulsew				
next	'at a time until it is zero			
'Initialize	Integral Control			
low KiInc 'initialize	increment control line			
low KiSelect	'select chip			
'reset the integral resistor to 0				
low KiUpDn	'increment resistance down to initialize			
for $x = 1$ to 99	resistor has 99 steps numbered 0-99			
pulsout Kilnc, pulsew 'step the re	•			
next	'at a time until it is zero			
'Computation of running average	e of the frequency			
check_frequency:	Estimate the input frequency			
pulsin pin,0,index	'count the zero crossings			
pulsin pin,1,x	'For frequency addition			
avg=index+x	'Assign the previous step frequency			
if avg > 5000 then set_constant	-			
if avg < 3070 then set_constant				
avg=avg/10	ω_mgn			
freq_measure=50000/avg*10	'10 times the measured frequency			
avg_freq_old=freq_round	To times the measured requestey			
avg = 7*avg_freq_old+freq_m	easure/8 '10 times cumulative frequency			
freq_round=avg	'10 times the running average			
x=freq_round//10	'Remainder after frequency truncation			
if x>9 then avg_freq_inc	'Rounding of frequency			
avg_freq=freq_round/10	'Average frequency			
Kp_old=Kp	'Store old Kp			
Ki_old=Ki	'Store old Ki			
if freq_round <> avg_freq_old				
gosub check_frequency	- · 			
6				

'Frequency rounding

avg_freq_inc: freq_round= freq_round+10

```
gosub check_frequency
set constants_low:
                                        'Constant Kp and Ki for f<100
  Kp=51
 Ki=1
gosub change_Kp
                                        'Constant Kp and Ki for f>163
set_constants_high:
 Kp=1
 K_{i=1}
gosub check_frequency
select_gains:
                                        'Subroutine for Gain selection
 index=avg freq-100
 'index vals [ 0 1 2 3 4 5 6 7 8 9 10 11 12 13 14 15 16 17 18 19 20 21 22 23 24 25
26 27 28 29 30 31 32 33 34 35 36 37 38 39 40 41 42 43 44 45 46 47 48 49 50 51 52 53 54
55 56 57 58 59 60 61 62 631
 lookup
3,53,53,53,53,53,52,52,51,51,51,50,50,50,49,49,49,48,48,48,47,47,46,46,45,45,45,44,43,
43,42,42,42,41,41,40,40],Kp
 lookup index, [1, 2, 2, 3, 3, 4, 5, 5, 6, 6, 7, 7, 8, 8,
9,10,10,10,11,11,12,13,14,14,15,15,16,17,17,18,18,19,19,20,21,21,22,22,23,23,24,24,25,
26,26,27,27,28,29,29,29,30,30,31,31,32,32,33,33,34,34,35,35,36],Ki
gosub change_Kp
change Kp:
                                        'Subroutine for changing Kp
 if Kp>Kp_old then increment_Kp
 if Kp<Kp_old then decrement_Kp
 if Kp=Kp_old then change_Ki
change_Ki:
                                        'Subroutine for changing Ki
 if Ki>Ki_old then increment_Ki
 if Ki<Ki_old then decrement Ki
 if Ki=Ki_old then check_frequency
increment_Kp:
                                        'Increase Kp from old value
 Kp_inc=Kp-Kp_old
             ____Set Proportional Control Gain
 ' set resistor to Kp
 low KpSelect
                                        'select chip
 high KpUpDn
                                        'increment resistance up to set value
 for x = 1 to Kp_inc
 pulsout KpInc, pulsew
 next
```

high KpSelect 'DeSelect chip gosub change_Ki

increment Ki: 'Increase Ki from old value

Ki_inc=Ki-Ki_old
'_____Set Integral Control Gain

low KiSelect 'select chip

' set resistor to Ki

high KiUpDn 'increment resistance up to set value

for x = 1 to Ki_inc pulsout KiInc, pulsew

next

high KiSelect 'Deselect chip

gosub check_frequency

decrement_Kp: 'Reduce Kp from old value

Kp_inc=Kp_old-Kp
'set resistor to Kp

low KpSelect 'select chip

low KpUpDn 'increment resistance up to set value

for x = 1 to Kp_inc pulsout KpInc, pulsew

next

high KpSelect 'DeSelect chip

gosub change_Ki

decrement_Ki: 'Reduce Ki from old value

Ki_inc=Ki_old-Ki 'set resistor to Ki

low KiSelect 'select chip

' set resistor to Ki

low KiUpDn 'increment resistance up to set value

for x = 1 to Ki_inc pulsout KiInc, pulsew

next

high KiSelect 'Deselect chip

gosub check_frequency

